

STRUCTURE AND EARLY SOOT OXIDATION PROPERTIES OF LAMINAR DIFFUSION FLAMES

A. M. El-Leathy, F. Xu and G. M. Faeth
Department of Aerospace Engineering
The University of Michigan
Ann Arbor, Michigan

INTRODUCTION

Soot is an important unsolved problem of combustion science because it is present in most hydrocarbon-fueled flames and current understanding of the reactive and physical properties of soot in flame environments is limited. This lack of understanding affects progress toward developing reliable predictions of flame radiation properties, reliable predictions of flame pollutant emission properties and reliable methods of computational combustion, among others. Motivated by these observations, the present investigation extended past studies of soot formation in this laboratory (refs. 1-12), to consider soot oxidation in laminar diffusion flames using similar methods, see ref. 13 for a detailed description of the study.

Early work showed that O_2 was responsible for soot oxidation in high temperature O_2 -rich environments (refs. 14-18). Subsequent work in high temperature flame environments having small O_2 concentrations (refs. 19 and 20), however, showed that soot oxidation rates substantially exceeded estimates based on the classical O_2 oxidation rates of Nagle and Strickland-Constable (ref. 14) and suggests that radicals such as O and OH might be strong contributors to soot oxidation for such conditions. Neoh et al. (refs. 20 and 21) subsequently made observations in premixed flames, supported by later work (refs. 22-25), that showed that OH was responsible for soot oxidation at these conditions with a very reasonable collision efficiency of 0.13. Subsequent studies in diffusion flames, however, were not in agreement with the premixed flame studies: they agreed that OH played a dominant role in soot oxidation in flames, but found collision efficiencies that varied with flame conditions and were not in good agreement with each other (refs. 26-30) or with Neoh et al. (refs. 20 and 21). One explanation for these discrepancies is that optical scattering and extinction properties were used to infer soot structure properties for the studies of refs. 26-30 that have not been very successful for representing the optical properties of soot, see refs. 2-4 and references cited therein. Whatever the source of the problem, however, these differences among observations of soot oxidation in premixed and diffusion flames clearly must be resolved. Motivated by these findings, the present study undertook measurements of soot and flame properties within the soot oxidation region of some typical laminar diffusion flames and exploited the new measurements to identify soot oxidation mechanisms for these conditions. Present considerations were limited to the early stages of soot oxidation (carbon consumption less than 70%) where reactions at the surface of primary soot particles dominate the process, rather than the later stages when particle porosity and internal particle oxidation become important as discussed by Neoh et al. (ref. 22).

EXPERIMENTAL METHODS

Measurements were obtained along the axes of nonpremixed laminar flames involving acetylene, ethylene, propylene and propane as the fuels burning in coflowing air at atmospheric pressure. The burner was directed vertically upward, to yield flames having luminous flame lengths of roughly 100 mm. The following measurements were made: soot volume fractions using deconvoluted laser extinction, flow temperatures using deconvoluted multiline emission, soot structure using thermophoretic sampling and TEM analysis, concentrations of major gas species using sampling and gas chromatography, concentrations of some radical species (H, OH and O) using the deconvoluted Li/LiOH atomic absorption technique and streamwise velocities using laser velocimetry.

RESULTS AND DISCUSSION

Soot and Flame Structure. All soot particles were the same as observed during earlier work in both laminar premixed and diffusion flames (refs. 1-12). They consisted of roughly spherical primary particles that were nearly monodisperse at each flame condition and collected into mass fractal aggregates having large variations of the number of primary particles per aggregate.

Present observations of flame structure were similar to earlier observations in laminar jet diffusion flames (refs. 2,3,11,12); a typical example is illustrated in Fig. 1. Flow velocities, u , increase with distance due to effects of buoyancy yielding a nonlinear variation of residence time with distance. Effects of radiant heat loss are substantial, yielding relatively flat temperature, T , distributions with maximum values well below adiabatic flame temperatures. Primary soot diameters, d_p , reach a maximum early in the soot formation region due to combined effects of soot nucleation, growth and oxidation. The original fuel disappears due to effects of decomposition, oxidation and soot formation (the last being relatively minor). Robust fuel-like species, however, persist throughout the soot formation region, e.g., C_2H_2 , C_2H_4 , CH_4 and H_2 . Concentrations of radicals, e.g., H , OH and O , increase as the flame sheet is approached. Unlike premixed flames where radical concentrations are nearly in thermodynamic equilibrium (ref. 10), however, radicals exhibit superequilibrium ratios generally in excess of 10 in the present diffusion flames.

Soot Surface Oxidation Rates. Measured soot surface oxidation rates were corrected for effects of soot growth using the expression based on the Colket and Hall (ref. 31) soot surface growth mechanism. No condition was considered, however, where the correction for soot growth was more than half the gross soot oxidation rate. Similar to Neoh et al. (refs. 21 and 22), present soot oxidation rates (corrected for soot growth) were converted into collision efficiencies (or reaction probabilities) based on kinetic theory estimates of the collision rates of a given gas species with the surface of primary soot particles, see refs. 13, 21 and 22 for detailed descriptions of computations of collision efficiencies.

Collision efficiencies for soot oxidation were found for O_2 , CO_2 , H_2O , O and OH , see ref. 13 for all these results; present results will be limited to collision efficiencies as a function of height for O_2 , CO_2 and OH as examples. The collision efficiencies of O_2 illustrated in Fig. 2 include the range of values measured by Neoh et al. (refs. 21 and 22) in premixed flames, the values found from the present experiments in diffusion flames, and values estimated from the predictions of Nagle and Strickland-Constable (ref. 14) for the conditions where present observations were made in diffusion flames. The Nagle and Strickland-Constable approach is known to be effective when soot oxidation is dominated by O_2 (i.e., when radical concentrations are small) and there are significant concentrations of O_2 along the present soot paths, see Fig. 1. Thus, the fact that Nagle and Strickland-Constable estimates of the O_2 collision efficiencies are 10-100 times smaller than present measurements strongly suggests that some other species is mainly responsible for soot oxidation in the present flames. The large scatter (nearly a range of 100) of the collision efficiencies for the flames illustrated in Fig. 2 also support the conclusion that O_2 is not the main oxidizing species of soot for the present flame environments.

The collision efficiencies of CO_2 for soot oxidation are plotted in Fig. 3. Results shown on the figure include the range of values observed by Neoh et al. (ref. 21) in premixed flames, and values from the present investigation in diffusion flames both considering and ignoring the contribution of O_2 (estimated using the correlation of ref. 14). Clearly, allowing for direct oxidation by O_2 has little effect on the collision efficiencies estimated in Fig. 3. In addition, the overall scatter of the CO_2 collision efficiencies approaches 1000 for the range of test conditions considered in Fig. 3. Taken together, these findings do not support CO_2 as a major contributor to soot oxidation in flames, either alone or in parallel with soot oxidation by O_2 . Similar considerations yielded the same finding for the collision efficiencies of H_2O and O .

Finally, the collision efficiencies of OH for soot oxidation are plotted in Fig. 4 in the same manner as the results for CO_2 in Fig. 3. Direct oxidation of soot by O_2 is not very

important for the present flames, as before. On the other hand, the combined results in premixed and diffusion flames exhibit rather small levels of scatter (roughly a factor of 3). Thus, the results in premixed and diffusion flames are in remarkably good agreement, e.g., the present mean OH collision efficiency in diffusion flames of 0.10 (with a standard deviation of 0.07) is not statistically different from the value of 0.13 measured by Neoh et al. (ref. 21) in premixed flames. These findings are helpful but the final stage of oxidation in diffusion flames (for carbon consumption larger than 70%), where primary particle porosity and internal particle oxidation become factors, must still be resolved.

ACKNOWLEDGMENTS

This research was sponsored by NASA Grant NAG3-1878 under the technical management of Z. G. Yuan of the National Center for Microgravity Research, NASA Glenn Research Center, Cleveland, Ohio.

REFERENCES

1. Sunderland, P.B., et al., *Combust. Flame* 96:97 (1994).
2. Sunderland, P.B., Köylü, Ü.Ö. and Faeth, G.M., *Combust. Flame* 100:310 (1995).
3. Sunderland, P.B. and Faeth, G.M., *Combust. Flame* 105:132 (1996).
4. Lin, K.-C., Sunderland, P.B. and Faeth, G.M., *Combust. Flame* 104:369 (1996).
5. Urban, D.L. et al., *AIAA J.* 36:1346 (1998).
6. Lin, K.-C. et al., *Combust. Flame* 116:415 (1999).
7. Lin, K.-C. and Faeth, G.M., *AIAA J.* 37:759 (1999).
8. Xu, F., Sunderland, P.B. and Faeth, G.M., *Combust. Flame* 108:1471 (1997).
9. Xu, F., Lin, K.-C. and Faeth, G.M., *Combust. Flame* 115:195 (1998).
10. Xu, F. and Faeth, G.M., *Combust. Flame* 121:640 (2000).
11. Xu, F. and Faeth, G.M., *Combust. Flame*, in press.
12. El-Leathy, A.M., Xu, F. and Faeth, G.M., *Combust. Flame*, in preparation.
13. Xu, F., El-Leathy, A.M. and Faeth, G.M., *Combust. Flame*, submitted.
14. Nagle, J. and Strickland-Constable, R.F., *Proc. Fifth Carbon Conf.* 1:154 (1962).
15. Rosner, D.E. and Allendorf, H.D., *AIAA J.* 6:658 (1968).
16. Wright, F.J., *Proc. Combust. Inst.* 15:1449 (1974).
17. Radcliffe, S.W. and Appleton, J.P., *Combust. Sci. Tech.* 4:171 (1971).
18. Park, C. and Appleton, J.P., *Combust. Flame* 20:369 (1973).
19. Fenimore, C.P. and Jones, C.W., *J. Phys. Chem.* 71:593 (1967).
20. Mulcahy, M.F.R. and Young, B.C., *Carbon* 13:115 (1975).
21. Neoh, K.G., Howard, J.B. and Sarofim, A.F., *Particulate Carbon* (D.C. Sieglä and B.W. Smith, ed.), Plenum Press, New York, 1980, p. 261.
22. Neoh, K.G., Howard, J.B. and Sarofim, A.F., *Proc. Combust. Inst.* 20:951 (1984).
23. Wicke, B.C., Wong, C. and Grady, K.A., *Combust. Flame* 66:37 (1986).
24. Wicke, B.C. and Grady, K.A., *Combust. Flame* 69:185 (1987).
25. Roth, P., Brandt, O. and von Gersum, S., *Proc. Combust. Inst.* 23:1485 (1990).
26. Garo, A., Lahaye, J. and Prado, G., *Proc. Combust. Inst.* 21:1023 (1986).
27. Garo, A., Prado, G. and Lahaye, J., *Combust. Flame* 79:226 (1990).
28. Puri, R., Santoro, R.J. and Smyth, K.C., *Combust. Flame* 97:125 (1994).
29. Puri, R., Santoro, R.J. and Smyth, K.C., *Combust. Flame* 102:226 (1995).
30. Hardiquert, M. et al., *Combust. Flame* 111:338 (1997).
31. Colket, M.B. and Hall, R.J., *Soot Formation in Combustion* (H. Bockhorn, ed.), Springer-Verlag, Berlin, 1994, p. 442.

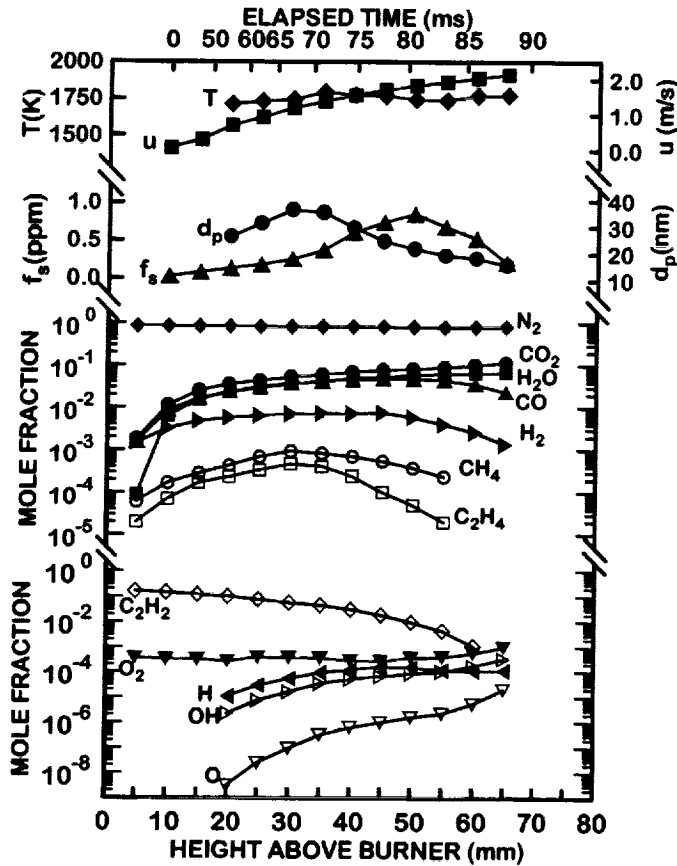


Fig. 1. Measured soot and flame properties along the axis of an acetylene/air laminar jet diffusion flame at atmospheric pressure.

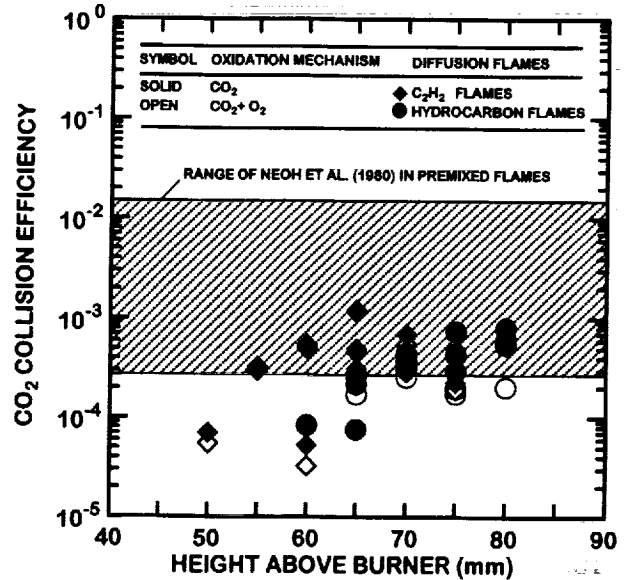


Fig. 3. Collision efficiencies assuming soot burnout due to attack by CO₂. Found from refs. 13 and 21.

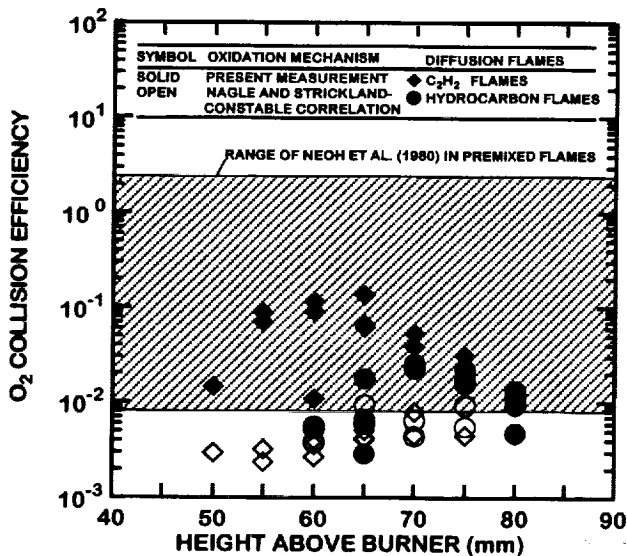


Fig. 2. Collision efficiencies assuming soot burnout due to attack by O₂. Found from refs. 13, 14 and 21.

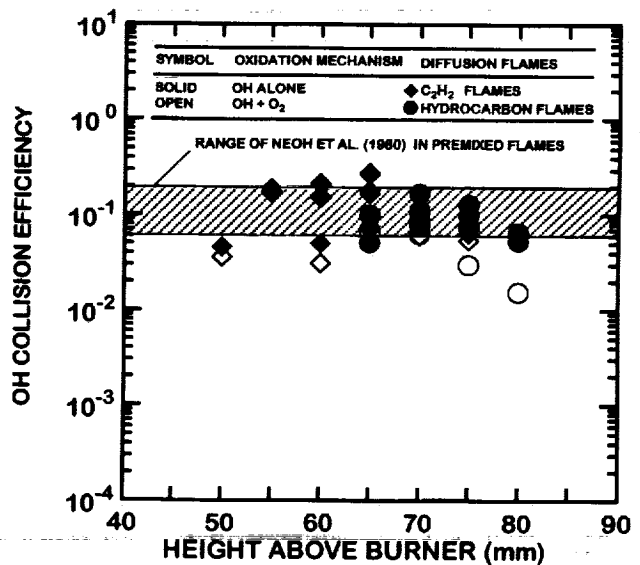


Fig. 4. Collision efficiencies assuming soot burnout due to attack by OH. Found from refs. 13 and 21.